



FCC–HCP phase boundary in lead

A. Kuznetsov^{a,*}, V. Dmitriev^a, L. Dubrovinsky^b, V. Prakapenka^c, H.-P. Weber^{a,d}

^aGroup “Structure of Materials under Extreme Conditions”, European Synchrotron Radiation Facility,
Swiss–Norwegian Beam Lines at ESRF, P.O. Box 220, F-38043 Grenoble, France

^bBayerisches Geoinstitut, Universitaet Bayreuth, D-95440 Bayreuth, Germany

^cANL/CARS, University of Chicago, 9700 S. Cass Avenue, Argonne, IL 60439, USA

^dInstitute of Crystallography, University of Lausanne, CH-1015 Lausanne, Switzerland

Received 8 February 2002; accepted 7 March 2002 by H. Eschrig

Abstract

The pressure–temperature phase diagram of Pb was mapped from synchrotron X-ray diffraction data measured to 40 GPa and 800 K, in the region including the hexagonal-close-packed to face-centered cubic transformation; the corresponding p – T – V equations of state were fitted for both phases. An unexpected interaction of Pb with NaCl surrounded the samples and significant reduction of the alloying temperature with Au was observed. © 2002 Elsevier Science Ltd. All rights reserved.

PACS: 61.66.Bi; 62.50. + p; 64.90. + b

Keywords: A. Metals; C. Crystal structure and symmetry; D. Phase transitions; E. High pressure

Elemental lead, one of the oldest metal known to man (mentioned in Exodus!), has many applications, some derived from its low tensile strength (shock absorbers in foundations of high-rise buildings), others from its high absorption of electromagnetic radiation (protective shielding), its high resistance to corrosion (economical plumbing), its easy alloyability (solder material)—to mention just a few key attractive properties. In everyday life, its economically most important use, however, comes from its favorable electrical properties; lead-acid storage batteries, the demise of which has been predicted for decades, are still being continuously improved. In its compounded form, the uses of lead are even more ubiquitous and therefore too numerous to mention here.

So lead is clearly, already in its elemental form, a material of strategic importance, and it is therefore surprising that the phase diagram of such an important element has been so cursorily explored till now. Only the melting curve has been mapped, first up to 9 GPa and 1200 K using DTA [1,2], and later on extended to 100 GPa and 4000 K [1,3] with laser heating. Isothermal high-pressure X-ray diffraction experiments first disclosed the transformation of Pb

from the face-centered cubic (FCC) form to the hexagonal-close-packed (HCP) structure at 14 GPa [4] and then, at about 120 GPa, to the body-centered cubic (bcc) phase [5,6]. However, the phase boundaries, phase coexistence regions and their evolution with an increase in temperature were not studied. In the present letter, we communicate the fcc-to-hcp transition region mapped to high temperature, and the corresponding pressure–temperature equation of state (EOS) of Pb metal.

In situ high-pressure–high-temperature data were obtained at the ID-30 beam line of the European Synchrotron Radiation Facility (ESRF, Grenoble, France) by angle-dispersive X-ray diffraction techniques employing monochromatic ($\lambda = 0.3738 \text{ \AA}$) X-radiation. Small pieces of polycrystalline Pb (99.999% purity, Advent) were studied in externally heated, gasketed diamond-anvill cell. The existence of reliable data on pressure–temperature EOS for NaCl [7] allowed us to use this material both as a pressure-transmitting medium and the pressure calibrant at high temperature. A K-type thermocouple placed close to the high-pressure sample chamber was used to measure the temperature of the sample. Diffraction measurements were performed up to a maximum pressure of 40 GPa and to a maximal temperature 800 K, these limits ensuring completion of the fcc-to-hcp transformation.

Fig. 1 shows the selected angle-resolved X-ray diffraction

* Corresponding author. Tel.: +33-476882079; fax: +33-476882694.

E-mail address: akuznets@esrf.fr (A. Kuznetsov).

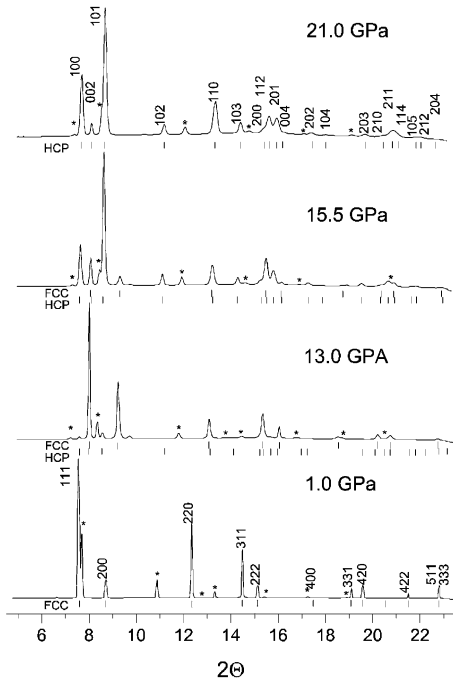


Fig. 1. Examples of high-pressure synchrotron radiation X-ray powder diffraction patterns of Pb metal in different phases at room temperature. * denote fcc NaCl peaks.

patterns of lead up to 21 GPa at ambient temperature, covering the transition region. Room-temperature results are in good agreement with the previous reports of Refs. [5,6]. All peaks could be indexed with the fcc, hcp structures of Pb and the fcc NaCl structure. At room temperature, the onset of the phase transition from the fcc phase to the hcp phase takes place at a pressure of about 12.0 GPa, where at least two diffraction peaks of the hcp Pb, 100 and 101, which do not overlap with fcc peaks, are observed (Fig. 1). With increasing pressure, the intensities of the hcp lines increase and the fcc lines disappear. The fcc-to-hcp transition in Pb is very sluggish, both the fcc and hcp phases coexist up to a pressure of 20 GPa.

The existence of a large two-phase region, observed also in preceding experiments on Pb [8], is consistent with a small volume reduction, $\Delta V/V$, at the fcc-to-hcp transition (Table 1) and thus a small free energy difference, ΔG , between fcc and hcp phases. The considerable difference

Table 1
Volume reduction at the fcc-to-hcp phase transition at different temperatures

T (K)	P (GPa)	V_{fcc} ($\text{\AA}^3 \text{ mol}^{-1}$)	V_{hcp} ($\text{\AA}^3 \text{ mol}^{-1}$)	$\Delta V/V$ (%)
296	13.1	25.12	24.84	1.02
402	13.9	25.14	24.92	0.89
469	12.6	25.26	25.06	0.77

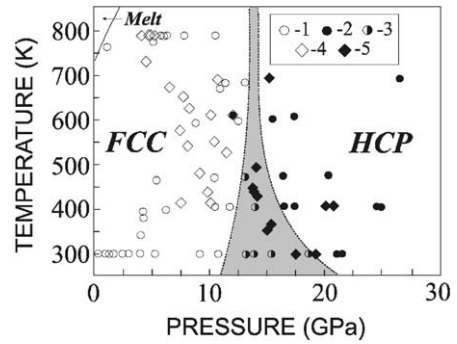


Fig. 2. P–T phase diagram of lead. Compression: 1, fcc phase; 2, hcp; 3, two-phase mixture. Decompression: 4, fcc; 5, hcp. Shaded is the two-phase region.

between ΔG and the activation energy (barrier) G_M of the martensitic fcc-to-hcp transformation results in a kinetic hysteresis of the transformation and the existence of a large two-phase region [9].

Fig. 2 shows the results of diffraction experiments and shows the phase diagram of the lead in the pressure range covering the fcc-to-hcp transformation region. One can see that the two-phase pressure range decreases with temperature increase, in full agreement with the kinetic interpretation of its nature. The progressive decrease of $\Delta V/V$ is characteristic for this pressure-induced transition with temperature increase (Table 1).

In order to obtain the p–T–V EOS for Pb, a series of isothermal equations of the Birch–Murnaghan form [10]:

$$P(V, T) = \frac{3}{2} B(T) (v^{7/3} - v^{5/3}) \left\{ 1 + \frac{3}{4} [B'(T) - 4] (v^{2/3} - 1) \right\} \quad (1)$$

with $v = V_0(T)/V$, were fitted to the experimental data. The incorporation of the temperature effect proceeds by the assumption of temperature dependence of the parameters of Eq. (1). First, the thermal expansion at ambient pressure should be taken into account:

$$\begin{aligned} V_0(T) &= V_0(T_0) \exp \left[\int_{T_0}^T \alpha(T) dT \right] \\ &= V_0(T_0) \exp \left[\int_{T_0}^T (\alpha_0 + \alpha_1 T + \alpha_2 T^2) dT \right] \\ &\cong V_0(T_0) \left(1 + \alpha_0 \tau + \frac{1}{2} \alpha_1 \tau^2 + \frac{1}{3} \alpha_2 \tau^3 \right), \end{aligned} \quad (2)$$

where $\tau = (T - T_0)$ with $T_0 = 296$ K. Then a simplest polynomial expansion in temperature can be applied to the bulk modulus B and its pressure derivative B' :

$$B(T) = B_0 + \beta_1 \tau + \beta_2 \tau^2; \quad B'(T) = B'_0 + \beta'_1 \tau. \quad (3)$$

Thus, $V_0, B_0, B'_0, \alpha_0, \alpha_1, \alpha_2, \beta_1, \beta_2, \beta'_1$ are the fitted parameters. Table 2 summarizes the numerical results of the

Table 2
Parameters for the p–T–V EOS of lead

Parameter	fcc	hcp
V_0 ($\text{\AA}^3 \text{mol}^{-1}$)	30.307	29.908
B_0 (GPa)	40.5	54.2
β_1	-1.07×10^{-3}	-5.46×10^{-2}
β_2	-1.14×10^{-5}	2.34×10^{-5}
B'_0	5.74	3.61
β'	-5.45×10^{-3}	5.01×10^{-3}
α_0	8.67×10^{-5}	8.97×10^{-5}
α_1	2.12×10^{-9}	2.52×10^{-8}
α_2	1.83×10^{-10}	0.0

fitting procedure. For both fcc and hcp phases the fitted equilibrium volume V_0 is close to that found in earlier experiments, bulk modulus and the pressure derivative of the bulk modulus are also in reasonably good agreement at 300 K [6,11]. Fig. 3 shows the fitted EOS curves plotted with experimental data scaled to the room temperature by Eqs. (2) and (3).

It is worthwhile to mention, in conclusion, some additional results concerning the interaction of the metal lead with some materials. First, we had to discard gold as the pressure calibrant because of its alloying with lead at surprisingly low temperature. A discontinuity in the diffraction patterns evolution of Pb related to the alloying process was observed, for example, at 460 K and 4.2 GPa. Another interesting reaction was observed when we used the Pb + NaCl mixture, even under moderate pressure in the vicinity of the melting curve. We succeeded in visualizing traces of PbCl_2 (Fig. 4), with lattice parameters $a = 6.4575(6)$ \AA , $b = 4.8139(6)$ \AA , $c = 9.9755(0)$ \AA ; this compound was

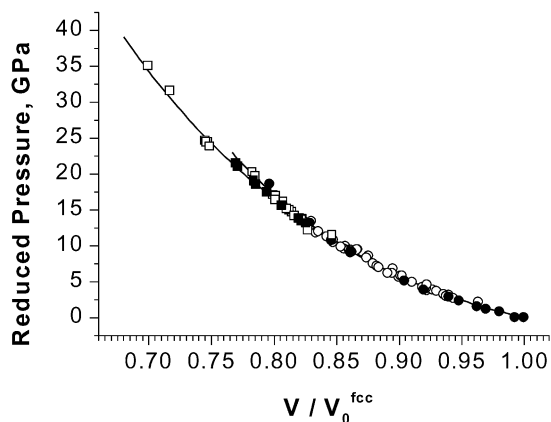


Fig. 3. Pressure–volume relations in Pb. Circles: fcc; squares: hcp. The solid symbols represent the room temperature results; the open symbols represent the reduced high-temperature data. The solid curves are the fits of the Birch–Murnaghan EOS with the parameters listed in Table 1.

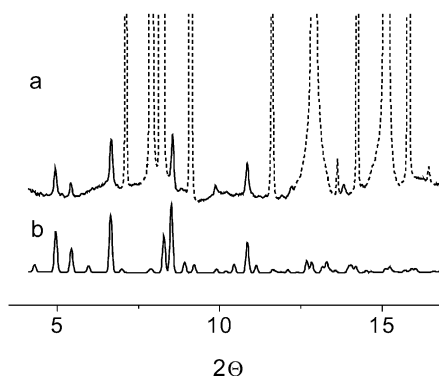


Fig. 4. Reaction of lead with NaCl. (a) X-ray powder diffraction of Pb with NaCl as pressure-transmitting medium at $p = 10.9$ GPa and $T = 663$ K. Dotted peaks correspond to fcc Pb and fcc NaCl. (b) Simulated powder diffraction pattern of PbCl_2 .

produced in the chemical reaction between the lead metal and sodium chloride. We could not determine the precise starting pressure of the reaction—only the pressure range (between ambient and 10.0 GPa). The controlled annealing of the Pb + NaCl mixture during 200 h at $T = 675$ K, close to the melting point, under ambient pressure did not affect the initial components.

In summary, we have studied the temperature evolution of the fcc-to-hcp transformation in lead metal and determined the p–T–V equations of state for the fcc and hcp phases up to 800 K and 40 GPa. We believe our results could be used for a pressure–temperature calibration scale in future high pressure–high temperature experiments.

References

- [1] D.A. Young, Phase Diagrams of Elements, University of California Press, Berkeley, 1991.
- [2] E.Yu. Tonkov, High Pressure Phase Transformations: A Handbook, vol. 2, Gordon & Breach, Philadelphia, 1992.
- [3] B.K. Godwal, C. Meade, R. Jeanloz, A. Garcia, A.Y. Lui, M.L. Cohen, Science 248 (1990) 462.
- [4] T. Takashi, H.K. Mao, W.A. Bassett, Science 165 (1969) 1352.
- [5] C.A. Vanderborgh, Y.K. Vohra, H. Xia, A.L. Ruoff, Phys. Rev. B 41 (1990) 7338.
- [6] H.K. Mao, Y. Wu, J.F. Shu, J.Z. Hu, R.J. Hemley, D.E. Cox, Solid State Commun. 74 (1990) 1027.
- [7] J.M. Brown, J. Appl. Phys. 86 (1999) 5801.
- [8] H.K. Mao, P.H. Bell, Yearbook, vol. 77, Carnegie Institute, Washington, 1978 p. 842.
- [9] J.W. Christian, The Theory of Phase Transformations in Metals and Alloys, Pergamon, New York, 1965.
- [10] F. Birch, J. Geophys. Res. 83 (1978) 1257.
- [11] Y.K. Vohra, A. Ruoff, Phys. Rev. B 42 (1990) 8651.